TEM-Assisted Fabrication of Sub-10 nm SECM Tips

Xiang Wang, †,§ Lili Han $^{\#}$ Huolin Xin $^{\#}$ and Michael V. Mirkin †,§,*

*Corresponding Author

E-mail: mmirkin@qc.cuny.edu

FAX: 718-997-5531

[†] Department of Chemistry and Biochemistry, Queens College, Flushing, NY 11367, USA

[§] The Graduate Center of CUNY, New York, NY 10016

[#] Department of Physics & Astronomy, University of California, Irvine, CA 92697.

ABSTRACT

High-resolution SECM is a powerful technique for mapping surface topography and reactivity on the nanoscale and investigating heterogeneous processes at the level of single nanoparticles. The ability to fabricate ultra-small nanoelectrode tips is critical for the progress in nano-SECM. Despite long-term efforts to improve previously developed procedures, the preparation and characterization of disk-type polished tips with the radius < ~25 nm remains challenging and unpredictable. One of the problems is that the geometry of such tips is hard to characterize by either SEM or AFM that have been employed for examination of somewhat larger nanoelectrodes. Herein, we report a new approach to more predictable and reproducible two-step fabrication of ultra-small (≤10 nm radius) polished Pt electrodes assisted by TEM imaging. Both voltammetric and SECM responses of the prepared nanoelectrodes are consistent with the size and geometry extracted from TEM images. These tips can be used to attain sub-10 nm spatial resolution of SECM imaging and kinetic studies.

A long-term quest to reduce the dimensions of electrochemical probes that began with the introduction of micrometer-sized ultramicroelectrodes in early 1980's continues to attract significant interest. Nanometer-sized electrochemical probes are essential for numerous applications, ranging from measurements of fast heterogeneous kinetics under steady-state conditions to high resolution electrochemical imaging and electrochemistry of single molecules. The smaller the electrode the more valuable tool it is for many of those applications. For instance, the mass-transfer rate at a disk-type nanoelectrode under steady state (and, therefore, the upper limit for the measurable heterogeneous rate constant) is inversely proportional to its radius. If a nanoelectrode is used as a scanning electrochemical microscopy (SECM) tip, its radius determines the spatial resolution of SECM imaging.

The difficulties in fabricating and characterizing nanoelectrodes increase exponentially with decreasing size. Using an established methodology based on pulling metal wires into glass capillaries with a laser pipette puller and mechanical polishing, 12,13 a skilled experimentalist can consistently fabricate good quality flat, disk-type electrodes with the radius, $a \ge 25$ -30 nm. The geometry of such electrodes can be characterized by various microscopic and electrochemical techniques, including scanning electron microscopy (SEM), $^{14-16}$ fast-scan voltammetry, 17 atomic force microscopy (AFM), 18 transmission electron microscopy (TEM), $^{19-21}$ and SECM. 13,22 By contrast, fabricating significantly smaller electrodes with $a \le 5$ -10 nm remains highly unpredictable, and the success rate is typically low. Electrodes of this size cannot be visualized by SEM or AFM, and electrochemical experiments carried out at a nanoelectrode without adequate characterization of its geometry are likely to be marred by artifacts and misinterpretations. 16,18,23 Sometimes, alternative strategies can be employed to avoid the need for ultra-small nanoelectrodes. For instance, relatively large tip electrodes with a small RG (RG

= r_g/a , i.e. the ratio of glass radius to that of the conductive tip) and ultra-flat substrates were used to create very thin nanogaps with well-defined geometry and measure fast electron-transfer rates.²⁴ This approach, however, is not suitable for other applications, where smaller tips are irreplaceable. For instance, ultra-small SECM tips must be employed to observe possible deviations from classical electrochemical theory at nanointerfaces,²⁵ image atomic-scale active sites on catalyst surfaces, or make analytical measurements in subcellular compartments.²⁶

The surface of a nanoelectrode after mechanical polishing is often recessed into the insulating glass, and consequently its apparent radius extracted from the diffusion current is much smaller than the true radius of the recessed conductive core. 18,23 This problem, which is not always apparent from SEM or AFM images, is easy to detect by TEM. For instance, in Fig. S1A, the true radius of the recessed disk in the TEM image is ~30 nm, while the apparent radius value of ~10 nm can be extracted from the corresponding steady-state voltammogram (Fig. S1B). Another common issue—nanoscale electrostatic damage¹⁶—may also be hard to detect by SEM or AFM if the defects in the glass insulator are on its side surface (Fig. S2A). The shape of the steady-state voltammogram is this case may also look normal ¹⁶ (Fig. S2B). TEM is a good technique for detecting such flaws in ultra-small nanoelectrodes. The pioneering work of the Zhang's group¹⁹ showed the possibility of TEM imaging 1-3 nm radius Pt wires sealed in glass. Such imaging is not straightforward when the insulator sheath is thick because the electron beam cannot penetrate thick layers of glass (e.g., $>1 \mu m$). In a small SECM nanotip, $r_g << 1 \mu m$, and TEM can provide detailed information about both metal core and glass sheath. Here, we introduce a two-step approach to TEM-assisted fabrication of sub-10 nm SECM tips. First, a slightly polished and presumably imperfect nanoelectrode is imaged with a TEM to evaluate its potential for becoming a well-shaped ultra-small tip. Then, another round of polishing and TEM

imaging produces a nanoelectrode with a desired size and shape for SECM experiments.

EXPERIMENTAL SECTION

Chemicals. Ferrocenemethanol (FcMeOH, 97%, Sigma-Aldrich) was sublimed before use. KCl (Sigma-Aldrich) was used as received. Aqueous solutions were prepared using deionized water with total organic carbon (TOC) < 1 ppb from the Milli-Q Advantage A10 system equipped with Q-Gard T2 Pak and a Quantum TEX cartridge.

Fabrication of nanoelectrodes. Pt nanoelectrodes were prepared by pulling and heat sealing 25 μm-diameter Pt wires (Goodfellow) into borosilicate glass capillaries (Drummond; o.d., 1.0 mm; i.d., 0.2 mm) under vacuum with a P-2000 laser pipette puller (Sutter Instrument Co.). The produced nanoelectrodes were polished on a 50 nm alumina pad (Precision Surfaces International) under video microscopic control. The electrodes were characterized by TEM imaging, steady-state voltammetry, and SECM. The appropriate protection was used to avoid electrostatic damage to the nanotips. ¹⁶

Voltammetry. A two-electrode cell was employed for electrochemical measurements with a nanoelectrode used as a working electrode and an Ag/AgCl wire serving as the reference. Voltammograms were obtained using a CHI 760 electrochemical workstation with a pA booster (CH Instruments). The current offset for the CHI 760E potentiostat, 1.8 pA, was subtracted from the measured current in all voltammograms and approach curves. All experiments were performed at room temperature (22-25 °C) inside a Faraday cage. The voltammograms were obtained with the scan rate of 100 mV/s.

SECM setup and procedures. SECM experiments were carried out using a home-built instrument similar to that described previously.⁹ All solutions contained 1mM FcMeOH as redox mediator and 0.1 M KCl supporting electrolyte. The substrate was always unbiased, and a

Pt wire was used as a counter electrode in positive feedback experiments. The tip was brought within $\sim 30~\mu m$ vertical distance from the substrate using a manual micromanipulator. Then the tip was moved toward the substrate using the z- piezo stage over $\sim 25~\mu m$ distance with a relatively large approach velocity (e.g., $0.5~\mu m/s$). To obtain an approach curve, the velocity was changed to a much slower value, e.g., $\sim 10~n m/s$. Theoretical approach curves were calculated with the a and RG values extracted from TEM images.

The tip/substrate alignment is a major challenge in SECM with ultra-small tips. The coarse leveling of the substrate was done by placing a bull's eye level on its stage. For the fine alignment, the tip was positioned above the substrate, ca. 2a away from its surface and scanned laterally along the x- or y- axis, over 200 nm in each direction, while monitoring the increase (or decrease) in the tip current (i_T). The tilt correction was performed by retracting the tip from the surface and adjusting the substrate angle with the positioning screws, as described previously.²⁸

Silicon chips and gold-coated glass slides were used as a substrate in SECM negative and positive feedback experiments, respectively. Before use, each substrate was subjected to simplified classical RCA clean to remove inorganic particles from its surface. Briefly, a slide was immersed in solution consisting of 5:1:1 deionized water, ammonia water (29% w.t.), and hydrogen peroxide (30%) at 75 °C for 10 min and then thoroughly rinsed with deionized water.

TEM characterization of nanoelectrodes. Pt nanoelectrodes were imaged using a field emission TEM (JEOL 2100F) operated at 200 keV. The electron beam intensity was adjusted to a desired magnitude to avoid melting the glass sheath; the maximum current density used was 12 electrons/Å²/s. A customized TEM holder (Fig. S3) allowed imaging a nanoelectrode before and after electrochemical experiments without cutting off its tip. Digital Micrograph software was used to measure the conductive tip diameter and RG.

RESULTS AND DISCUSSION

After pulling a metal microwire into a glass capillary, it is usually encased in glass. From the TEM image in Fig. 1 one can see some issues responsible for the low success rate and poor reproducibility in fabrication of ultra-small nanoelectrodes. The sealed Pt nanowire is discontinuous near the tip of the capillary, and its diameter varies dramatically along the electrode axis. If such an electrode was polished to remove a portion of glass adjacent to the tip shorter than that corresponding to cross-section 1 (indicated by a dashed red line in Fig. 1), it would yield no electrochemical signal because of the gaps in the Pt core. If the polishing stopped at a thicker part of the Pt wire (e.g., at cross-section 2), the resulting electrode would have a diameter of ~100 nm. The chances for this capillary to be polished up to cross-section 3, where Pt is thin, producing a ~10-nm-diameter tip are very low.

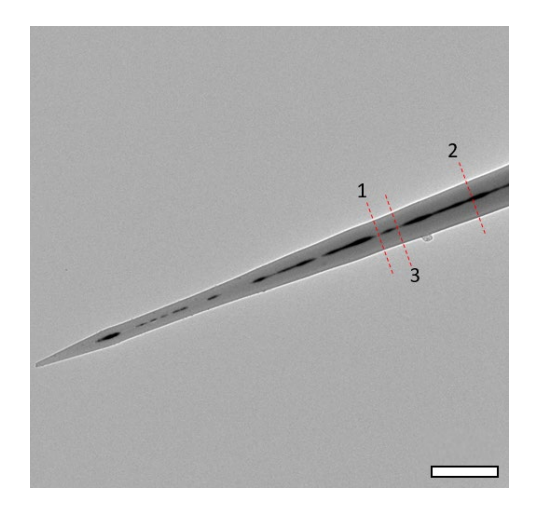


Figure 1. TEM image of Pt wire pulled into a glass capillary before polishing. Scale bar is 1 μm.

Having a relatively long portion of the sealed wire with a sufficiently small diameter greatly increases the probability of fabricating a small nanoelectrode. Using the two-step fabrication protocol, the pulled capillary is first gently polished, keeping a significant distance between the tip and the polishing surface. (Harsh initial polishing is likely to yield a large radius.) After initial polishing, the metal surface is typically recessed into glass insulator. A

TEM image obtained at this stage (Fig. 2A) can be used to verify that the wire is uniform, well-sealed in glass, and suitable for preparing a nanoelectrode with the desired a and RG. The corresponding voltammogram (Fig. 2C) shows that the Pt wire is continuous, though no wave of FcMeOH oxidation could be obtained at this deeply recessed electrode. The second polishing step yielded a disk-type electrode with $a \approx 10$ nm and RG ≈ 7 whose Pt surface is flush with glass (Fig. 2B). A similar radius value (a = 10.3 nm) was extracted from the corresponding steady-state voltammogram (Fig. 2D) using Eq. (1)

$$i_{T,\infty} = 4FDca \tag{1}$$

where $i_{T,\infty}$ is the diffusion limiting current, F is the Faraday constant, $c = 10^{-3}$ mol/cm³ and $D = 7.8 \times 10^{-6}$ cm²/s ¹³ are the bulk concentration and diffusion coefficient of FcMeOH, respectively. The longer the portion of the sealed metal wire with a sufficiently small diameter the higher the probability of fabricating a sub-10 nm electrode; however, polishing away a submicrometer long piece of the sealed capillary is technically challenging.

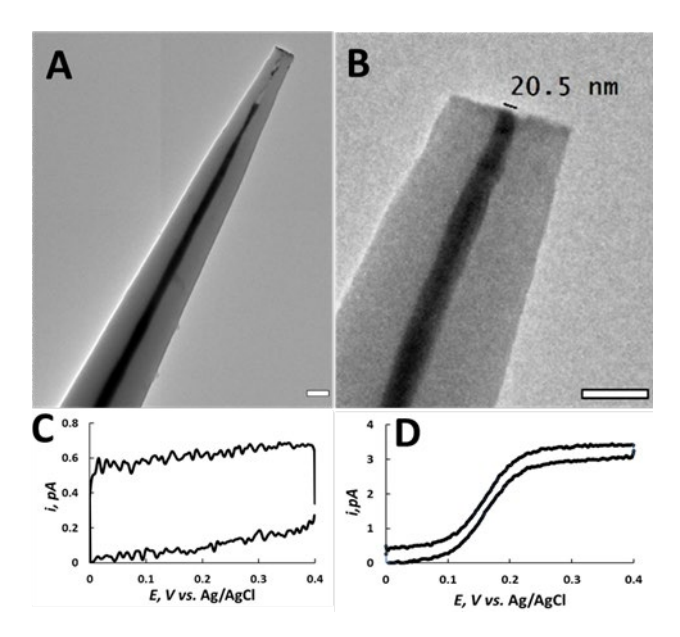


Figure 2. Two-step TEM assisted fabrication of Pt tip. Images of the nanoelectrode after the initial (A) and final (B) polishing. The corresponding steady-state voltammograms of the same tip are shown in panels (C) and (D), respectively. Scale bar is 200 nm (A) and 100 nm (B).

A smaller Pt tip with the radius ~7 nm is shown in Figs. 3A and 3B. The a value obtained from the steady-state voltammogram (Fig. 3C; $i_{T,\infty} = 2.0$ pA) is 6.7 nm in agreement with the TEM image. The glass surface looks flat and well-polished, though the RG \approx 15 is a little large for an SECM tip. Nevertheless, when this nanoelectrode was used as an SECM tip to approach an insulating substrate, the experimental current-distance curve (symbols in Fig. 3D) fitted well the theory for the normalized distance (d/a) values down to ~0.5, corresponding to d = 3.5 nm.

A more stringent test of the tip geometry is to approach a conductive substrate.¹³ While, an essentially normal current-distance curve in agreement with the theory for the pure negative SECM feedback can be recorded using a slightly recessed tip, when the feedback is positive,

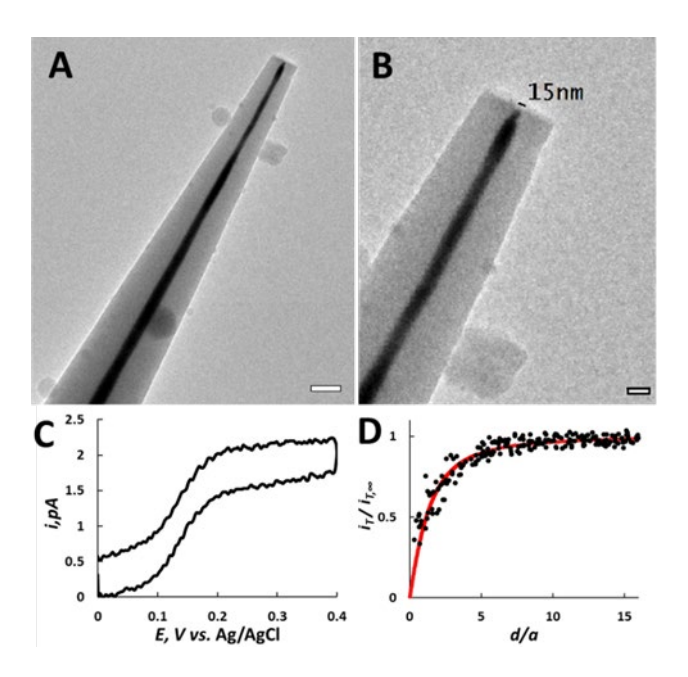


Figure 3. Characterization of a 7-nm-radius polished nanoelectrode. (A) Larger scale TEM image and (B) blowup of the nanotip. (C) Steady-steady state voltammogram of 1 mM FcMeOH at the same nanoelectrode. (D) Experimental approach curve (symbols) fitted to the SECM theory for pure negative feedback (solid line²⁷). a = 6.7 nm; RG = 15. The approach velocity was 10 nm/s. Scale bar is (A) 200 nm, (B) 50 nm.

a good fit can only be obtained if the recess depth is negligibly small. A 4.3-nm-radius nanoelectrode imaged in Fig. 4A was used to approach an Au-coated slide in solution containing 1 mM FcMeOH (Fig. 4B). The experimental approach curve (solid line) fits the theory reasonably well for $d/a > \sim 0.5$, corresponding to the separation distance ≥ 2 -3 nm, but the noise greatly increases at $d < \sim 6$ nm. As discussed previously, ¹³ this phenomenon is due to electron tunneling between the tip and conductive substrate. At a separation distance of a few nm, the large time variations in the tunneling current are due to piezo oscillations. At d < 2-3 nm, the tunneling current increases dramatically, producing the overflow of the potentiostat amplifier (inset in Fig. 4B). This picture is markedly different from the recently reported "electrochemical tunneling" between the tip and metal nanoparticle attached to an insulating substrate. ²⁸ In the latter case, the current measured in the tunneling mode was limited by diffusion of redox species to the nanoparticle. Here, the conductive substrate is macroscopic, and the tunneling current is very large. One should notice that the transition from conventional positive feedback response to tunneling regime is only possible if the electrode surface is not recessed into glass.

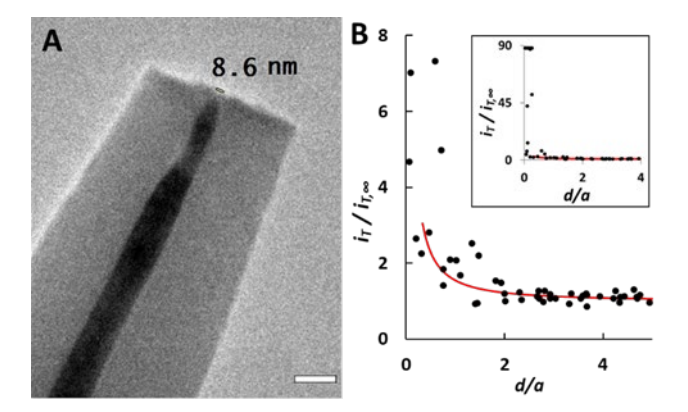


Figure 4. (A) TEM image of a 4.3-nm-radius polished nanoelectrode and (B) approach curve obtained with the same electrode used as an SECM tip. The experimental i_T -d curve (symbols) is fitted to the theory for pure positive feedback (solid line²²). a = 4.3 nm; RG = 22. The approach velocity was 10 nm/s. The inset in (B) shows the same approach curve on a larger current scale, including the overflow due to electron tunneling. Scale bar is 50 nm.

Each TEM image in Figs. 1-4 shows a particular two-dimensional projection of the tip. Because the nanoelectrode geometry is not perfectly axisymmetric, the tip radius, recess depth and r_g may look different in other 2D projections. A more complete picture of the tip geometry can be obtained by electron tomography.²⁹ The three-dimensional reconstruction of the nanotip is essential for elucidating complicated internal structures, such as carbon nanocavities,²⁹ but for more routine characterization of a disk-type electrode this laborious and complicated process is an overkill. A good compromise is to rotate a nanoelectrode inside the TEM and obtain several 2D projections (Figs. 5A-C). The three projections in Fig. 5 show essentially similar images of the \sim 3.5-nm-radius tip whose surface is flush with well-polished glass. Similar to the above

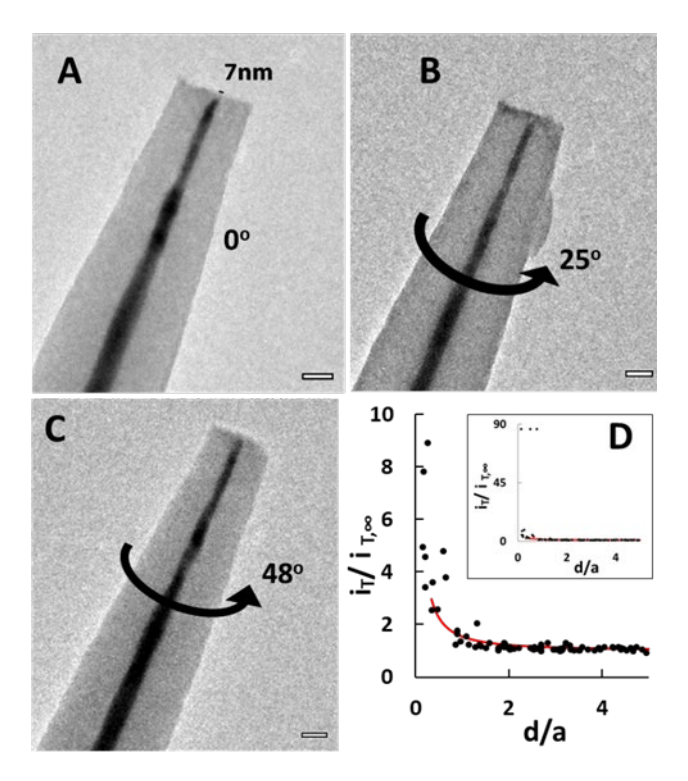


Figure 5. TEM images of the 7 nm Pt tip obtained at different rotation angles: (A) 0°, (B) 23°, and (C) 48° counterclockwise. (D) SECM current-distance curve obtained with the same tip approaching an Au-coated slide. Experimental data (symbols) is fitted to the positive feedback theory (solid line²²). The insert shows the same approach curve on a larger scale, including the current overflow caused by tunneling between the tip and Au substrate. The approach velocity was 10 nm/s. All scale bars are 50 nm.

12

discussion, the theoretical approach curve (solid line in Fig.5D) calculated for the pure positive

feedback with a = 3.5 nm is in agreement with the experimental data (symbols) at d/a > 0.5,

and the onset of tunneling results in the current overflow (see the inset).

In conclusion, the fabrication of sub-10 nm SECM tips has up to now been unpredictable,

uncontrollable, and completely irreproducible. The geometry of such a nanoelectrode must be

thoroughly characterized before using it in SECM experiments. The two-step TEM-assisted

fabrication protocol discussed in this Letter should allow ultra-small tips to be produced more

predictably and with a reasonably high success rate, thus enabling SECM imaging and kinetic

studies on the sub-10 nm scale.

■ ASSOCIATED CONTENT

Supporting Information

TEM images of deeply recessed and electrostatically damaged nanoelectrodes and corresponding

steady-state voltammograms. This material is available free of charge via the Internet at

http://pubs.acs.org.

■ AUTHOR INFORMATION

Corresponding Author

*E-mail: mmirkin@qc.cuny.edu. Fax: 718-997-5531.

Author Contributions

All authors have given approval to the final version of the manuscript.

Notes

The authors declare no competing financial interest.

■ ACKNOWLEDGMENTS

The support of this work by the National Science Foundation (CHE-1763337, MVM; CHE-1900401, HX) is gratefully acknowledged. This research used resources of the Center for Functional Nanomaterials, which is a U.S. DOE Office of Science Facility, at Brookhaven National Laboratory under Contract No. DE-SC0012704.

■ REFERENCES

- (1) Wightman, R. M.; Wipf, D. O. Voltammetry at Ultramicroelectrodes, in *Electroanalytical Chemistry*; Bard, A. J., Ed.; Marcel Dekker: New York, 1989; Vol. 15, pp 267-353.
- (2) Mirkin, M. V. Nanoelectrodes and liquid/liquid nanointerfaces, in *Nanoelectrochemistry* (Mirkin, M. V., Amemiya, S., Eds); CRC Press/Taylor & Frances, 2015, pp 539-572.
- (3) Oja, S. M.; Fan, Y.; Armstrong, C. M.; Defnet, P.; Zhang, B. Nanoscale Electrochemistry Revisited. *Anal. Chem.* **2016**, *8*, 414-430.
- (4) Wang, Y.; Velmurugan, J.; Mirkin, M. V. Kinetics of Charge-Transfer Reactions at Nanoscopic Electrochemical Interfaces. *Isr. J. Chem.* **2010**, *50*, 291-305.
- (5) Chen, R.; Nioradze, N.; Santhosh, P.; Li, Z.; Surwade, S. P.; Shenoy, G. J.; Parobek, D. G.; Kim, M. A.; Liu H.; Amemiya, S. Ultrafast Electron Transfer Kinetics of Graphene Grown by Chemical Vapor Deposition. *Angew. Chem., Int. Ed.* **2015**, *54*, 15134–15137.
- (6) Yu, Y.; Sun, T.; Mirkin, M.V. Toward more reliable measurements of electron-transfer kinetics at nanoelectrodes: next approximation. *Anal. Chem.* **2016**, *88*, 11758-11766.
- (7) Amemiya, S. Nanoscale Scanning Electrochemical Microscopy. In *Electroanalytical Chemistry, Vol. 26* (Bard, A. J.; Zoski, C. G., Eds.), CRC Press: 2015; pp 1-72.
- (8) Kai, T.; Zoski, C. G.; Bard, A. J. Scanning electrochemical microscopy at the nanometer level. *Chem. Commum.* **2018**, *54*, 1934-1947.
- (9) Sun, T.; Zhang, H.; Wang, X.; Liu, J.; Xiao, C.; Nanayakkara, S. U.; Blackburn, J. L.; Mirkin, M. V.; Miller, E. M. Nanoscale mapping of hydrogen evolution on metallic and semiconducting MoS₂ nanosheets. *Nanoscale Horiz.* **2019**, *4*, 619-624.
- (10) Fan, F. R. F.; Bard, A. J. Electrochemical Detection of Single Molecules. *Science* **1995**, 267, 364-367.
- (11) Bard, A. J.; Faulkner, L. R. Electrochemical Methods Fundamentals and Applications. 2nd Ed; Wiley & Sons, 2001, p. 360.
- (12) Shao, Y.; Mirkin, M. V.; Fish, G.; Kokotov, S.; Palanker, D.; Lewis, A. Nanometer-Sized Electrochemical Sensors. *Anal. Chem.* **1997**, *69*, 1627-1634.
- (13) Sun, P.; Mirkin, M. V. Kinetics of Electron Transfer Reactions at Nanoelectrodes. *Anal. Chem.* **2006**, *78*, 6526-6534.
- (14) Zhang, B.; Galusha, J.; Shiozawa, P. G.; Wang, G.; Bergren, A. J.; Jones, R. M.; White, R. J.; Ervin, E. N.; Cauley, C. C.; White, H. S. Bench-Top Method for Fabricating Glass-Sealed Nanodisk Electrodes, Glass Nanopore Electrodes, and Glass Nanopore Membranes of Controlled Size. *Anal. Chem.* 2007, 79, 4778-4787.

- (15) Agyekum, I.; Nimley, C.; Yang, C.; Sun, P. Combination of Scanning Electron Microscopy in the Characterization of a Nanometer-Sized Electrode and Current Fluctuation Observed at a Nanometer-Sized Electrode. *J. Phys. Chem. C* **2010**, *114*, 14970–14974.
- (16) Nioradze, N.; Chen, R.; Kim, J.; Shen, M.; Santhosh, P.; Amemiya, S. Origins of nanoscale damage to glass-sealed platinum electrodes with submicrometer and nanometer size. *Anal. Chem.* **2013**, *85*, 6198-6202.
- (17) Watkins, J. J.; Chen, J.; White, H. S.; Abruña, H. D.; Maisonhaute, E.; Amatore, C. Zeptomole Voltammetric Detection and Electron-Transfer Rate Measurements Using Platinum Electrodes of Nanometer Dimensions. *Anal. Chem.* 2003, 75, 3962-3971.
- (18) Nogala, W.; Velmurugan, J.; Mirkin, M. V. Atomic force microscopy of electrochemical nanoelectrodes. *Anal. Chem.* **2012**, *84*, 5192-5197.
- (19) Li, Y., Bergman, D.; Zhang, B. Preparation and electrochemical response of 1–3 nm Pt disk electrodes. *Anal. Chem.* **2009**, *81*, 5496-5502.
- (20) Zhou, M.; Yu, Y.; Hu, K.; Xin, H.; Mirkin M. V. Collisions of IrO_x Nanoparticles with Carbon Nanopipettes: Experiments with One Nanoparticle. *Anal. Chem.* **2017**, *89*, 2880–2885.
- (21) Wilde, P.; Quast, T.; Aiyappa, H. B.; Chen, Y. T.; Botz, A.; Tarnev, T.; Marquitan, M.; Feldhege, S.; Lindner, A.; Andronescu, C.; Schuhmann, W. Towards Reproducible Fabrication of Nanometre-Sized Carbon Electrodes: Optimisation of Automated Nanoelectrode Fabrication by Means of Transmission Electron Microscopy. *ChemElectroChem*, **2018**, *5*, 3083-3088.
- (22) Mirkin, M. V.; Fan, F.- R. F.; Bard, A. J. Scanning Electrochemical Microscopy. 13. Evaluation of the Tip Shapes of nm-Size Microelectrodes. *J. Electroanal. Chem.* **1992**, *328*, 47-62.
- (23) Baranski, A. S. On Possible Systematic Errors in Determinations of Charge Transfer Kinetics at Very Small Electrodes. *J. Electroanal. Chem.* **1991**, *307*, 287-292.
- (24) Najarian, A. M.; Chen, R.; Balla, R. J.; Amemiya, S.; McCreery, R. L. Ultraflat, Pristine and Robust Carbon Electrode for Fast Electron Transfer Kinetics. *Anal. Chem.* **2017**, *89*, 13532–13540.
- (25) Sun, Y.; Liu, Y.; Liang, Z.; Xiong, L.; Wang, A.; Chen, S. On the Applicability of Conventional Voltammetric Theory to Nanoscale Electrochemical Interfaces. *J. Phys. Chem. C* **2009**, *113*, 9878-9883.
- (26) Ying, Y. L.; Ding, Z.; Zhan, D.; Long, Y. T. Advanced electroanalytical chemistry at nanoelectrodes. *Chem. Sci.* **2017**, *8*, 3338-3348.
- (27) Cornut, R.; Lefrou, C. A unified new analytical approximation for negative feedback currents with a microdisk SECM tip. *J. Electroanal. Chem.* **2007**, *608*, 59–66.
- (28) Sun, T.; Wang, D.; Mirkin, M.V. Tunneling mode of scanning electrochemical microscopy: probing electrochemical processes at single nanoparticles. *Angew. Chem. Int. Ed.* **2018**, 57, 7463-746.
- (29) Hu, K.; Wang, D.; Zhou, M.; Bae, J. H.; Yu, Y.; Xin, H.; Mirkin M. V. Ultrasensitive Detection of Dopamine with Carbon Nanopipettes. *Anal. Chem.* **2019**, *91*, 12935–12941.

TOC graphic

